

Relativistic MHD jets and the GRBs

Christian Fendt

*Institut für Physik, Universität Potsdam
Am Neuen Palais 10
D-14469 Potsdam, GERMANY*

1 Introduction – astrophysical jets

High velocity highly collimated beams of plasma – the jets – are known as a general phenomenon among astrophysical sources of different energy and spatial scales. At the upper end of the scale are the extragalactic jets emanating from active galactic nuclei. Little brothers of extragalactic jets has been detected recently as Galactic superluminal sources – the so-called microquasars [1]. These jets originate in stellar mass black hole accretion disks in high-energy binary systems. Protostellar jets are non-relativistic with velocities of several 100 km/s [2].

The idea of a common astrophysical jet formation scenario is motivated by the observational fact that jet formation is always connected to (i) the existence of (strong) *magnetic fields* and (ii) the presence of an *accretion disk*. The magnetohydrodynamic (MHD) model of jet formation (cf. [3, 4]) allows to describe the various scales of astrophysical jets by a scaling of the jet *magnetization*. The theory tells us that highly relativistic jets must be also highly magnetized [5] and that rotating MHD flows are subject of a *self-collimation* process [6, 7]. In this paper, we ask whether the ultra-relativistic motion and strong collimation indicated for GRBs is achieved by a mechanism similar to the “classical” astrophysical jets.

2 Magnetohydrodynamic jets

Highly relativistic MHD jets originate in the accretion disk surrounding a central black hole (Fig. 1). The disk provides the Poynting flux and drives the electric current system. The jet is initiated as a slow wind from the inner disk by a process which is not yet completely understood, in particular its time-dependent character. Most probably, some disk instability is responsible for the ejection of knots perpendicular to the disk surface. The disk wind is first launched magneto-centrifugally [3] and further accelerated and collimated into a narrow beam by Lorentz forces. The parallel component $\vec{F}_{L,\parallel} \sim \vec{j}_\perp \times \vec{B}_\phi$ is accelerating (or decelerating), while the perpendicular force $\vec{F}_{L,\perp} \sim \vec{j}_\parallel \times \vec{B}$ is the collimating component (Fig. 1). Theoretical modeling,

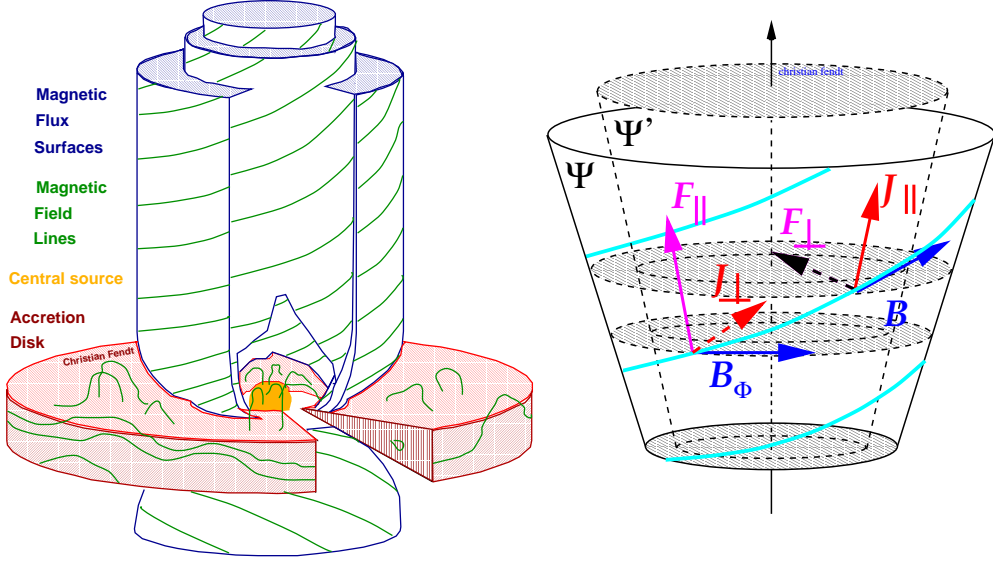


Figure 1: (*Left*) The model of MHD jets launched from an accretion disk surrounding the central mass. (*Right*) The accelerating and collimating Lorentz force components are projected with respect to the magnetic flux surfaces $\Psi(R, Z)$.

therefore, requires to solve the governing MHD equations. In this contribution, we will concentrate on solutions to the *stationary, axisymmetric, ideal MHD* equations in the relativistic limit. The advantage of the stationary model is the possibility to obtain *global* solutions for the jet structure on spatial scales and resolution which cannot (yet) be reached by time-dependent simulations [8, 9]. Long-term MHD simulations can, however, demonstrate the self-collimation of MHD jets (Fig.2; [7]).

2.1 Relativistic stationary MHD

The axisymmetric stationary ideal MHD equations can be reduced into two governing equations – the *Grad-Shafranov* equation (GSE) describing the force-balance across the magnetic flux surfaces¹ $\Psi(r, \theta)$ and the *wind equation* (WE) considering the forces along the field. Both equations are interrelated, however, in the relativistic limit of a high magnetization the field structure is almost force-free and can be investigated independently of the flow dynamics. Here, we will discuss solutions of the force-free GSE in Kerr metric appropriate for jets from rotating black holes,

$$\tilde{\omega} \nabla \cdot \left(\alpha \frac{1 - (\tilde{\omega}/\tilde{\omega}_L)^2}{\tilde{\omega}^2} \nabla \Psi \right) = \tilde{\omega} \frac{\omega - \Omega_F(\Psi)}{\alpha c^2} |\nabla \Psi|^2 \frac{d\Omega_F(\Psi)}{d\Psi} - \frac{1}{\alpha \tilde{\omega}} \frac{2}{c^2} I(\Psi) \frac{dI(\Psi)}{d\Psi} \quad (1)$$

¹ The magnetic flux is $\Psi(r, \theta) = (1/2\pi) \int \vec{B}_P \cdot d\vec{A}$. In general relativity, the integration is over a loop of the Killing vector $\vec{m} = \tilde{\omega}^2 \nabla \phi$. In Minkowski space the flux is integrated over a circular area around the symmetry axis.

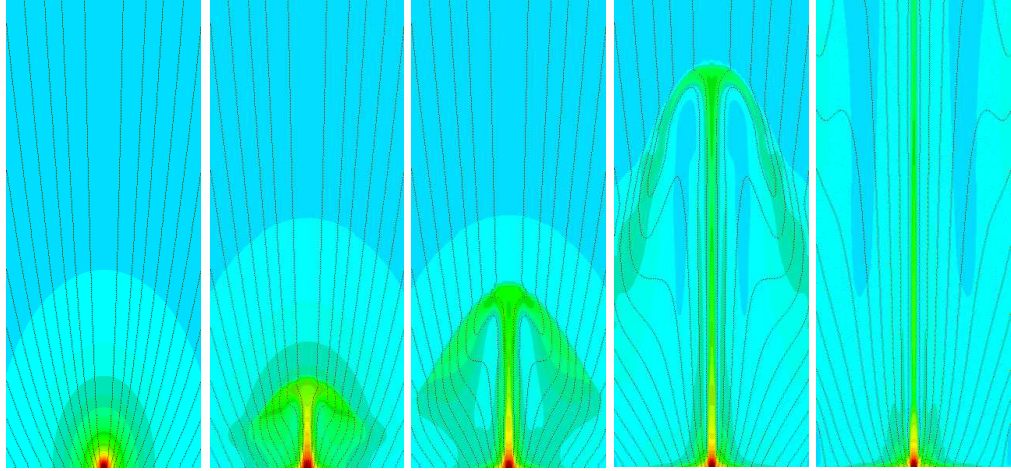


Figure 2: Non-relativistic MHD simulations of jet formation. Density (colors) and poloidal magnetic field lines after 0, 50, 100, 200 and 400 inner disk rotations.

(see [10]). In Eq. (1), ω is the angular velocity of a zero angular momentum observer (ZAMO), α the lapse of ZAMO proper time to the global time, $\tilde{\omega}$ the cylindrical radius, and $\tilde{\omega}_L(\Psi)$ the position of the two light “cylinders” (l.c.). $\Omega_F(\Psi)$ can be considered as rotational velocity of magnetic field lines. $I(\Psi)$ is the total poloidal electric current. The general relativistic *wind equation* for the poloidal velocity $u_p \equiv \Gamma v_p/c$ is² [4, 11, 12]

$$u_p^2 + 1 = \left(\frac{E}{\mu} \right)^2 \frac{k_0 k_2 - 2k_2 M^2 - k_4 M^4}{(k_0 - M^2)^2}, \quad (2)$$

with the Alfvén Mach number M . Specific total energy and angular momentum density $E(\Psi)$, $L(\Psi)$, are conserved quantities along Ψ . As a key parameter for MHD jets, the magnetization $\sigma(\Psi)$ measures the Poynting flux in terms of mass flux,

$$\sigma = \frac{\Phi^2 \Omega_F^2}{4 \dot{M} c^3}, \quad (3)$$

with the magnetic flux function $\Phi = B_P R^2$ and the mass flux \dot{M} . The launching of a relativistic jet requires at least one of three conditions – rapid rotation, strong field, or low mass load (Eq. 3). In general, *relativistic jets are highly magnetized* [13, 4, 5]. Fixing the field distribution, one finds a relation between the asymptotic Lorentz factor Γ_∞ and σ . We have (Michel-scaling) $\Gamma_\infty = \sigma^{1/3} \simeq (\Omega_F^2 \Phi^2 / \dot{M}_{jet})^{1/3}$ for a spherical flow with negligible gas pressure (“cold”) [13]. In the case of *collimation*, the power law index is different. If the magnetic flux surfaces open up faster than spherically radial, the asymptotic flow is dominated by kinetic energy [14].

² with the following abbreviations, $k_0 \equiv g_{33} \Omega_F^2 + 2g_{03} \Omega_F + g_{00}$, $k_2 \equiv 1 - \Omega_F(L/E)$, and $k_4 \equiv -(g_{33} + 2g_{03}(L/E) + g_{00}(L/E)^2) / (g_{03}^2 - g_{00}g_{33})$

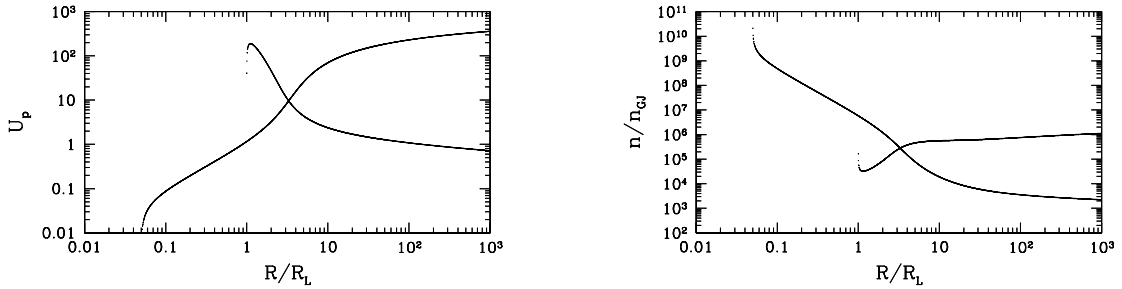


Figure 3: Solution of the relativistic MHD wind equation. Poloidal velocity u_P and particle density n over Goldreich-Julian density n_{GJ} versus radius. At the fast magnetosonic point, $R = 33R_L$, both solution branches intersect.

3 MHD jets in GRBs – structure and dynamics

3.1 Parameter estimates

We now estimate MHD jet parameters in the framework of GRBs assuming that these jets originate close to a stellar mass black hole and reach Lorentz factors up to 1000.

Disk magnetic field: Differential rotation amplifies the toroidal field up to equipartition, $B_\phi < B_{eq}$. A disk dynamo may amplify poloidal fields up to $B_P < B_\phi$. In advection dominated disks, $B_{eq} \simeq 10^9 G (M/5M_\odot)^{-1/2} (\dot{M}_a/\dot{M}_E)^{1/2} (R/3r_g)^{-5/4}$, with central mass M , accretion rate \dot{M}_a in terms of Eddington \dot{M}_E , and the horizon at r_g [15]. GRB models considering $10^{15} G$ fields are not consistent with this estimate.

Light cylinder: The l.c. of the jet magnetosphere is located at $R_L \simeq c/\Omega_F \simeq 4 \times 10^6 \text{ cm } (M/5M_\odot)$ if the jet originates just outside the marginally stable orbit.

Magnetization: The upper limit magnetization can be derived assuming the jet origin at the marginally stable orbit (highest field strength, most rapid disk rotation). Jet mass flow rates $\sim 10^{-11} M_\odot \text{ yr}^{-1}$ are indicated by GRB afterglows constraining the baryonic “jet” mass to $10^{-4} M_\odot$. This gives a jet magnetization of about 10^4 .

3.2 Acceleration – asymptotic Lorentz factor

Figure 2 shows a solution of the cold relativistic MHD WE in the Minkowski limit³ ($\sigma = 1000$, $Z(R) \sim R^{1.8}$). The flow accelerates rapidly, becomes super Alfvénic ($R > R_L$), super fast magnetosonic ($R > 33R_L$) and reaches asymptotically $u_P \sim 300$. The density remains above the Goldreich-Julian density, confirming the underlying *MHD assumption* a posteriori. For cold jets, σ is a free parameter. Thus, we may investigate the jet dynamics for different magnetization (Fig. 3). The two chosen flux distributions deviate from a spherical flow and indicate the modified Michel-scaling.

³ For hot wind solutions considering the influence of Kerr metric on the jet acceleration, see [12]

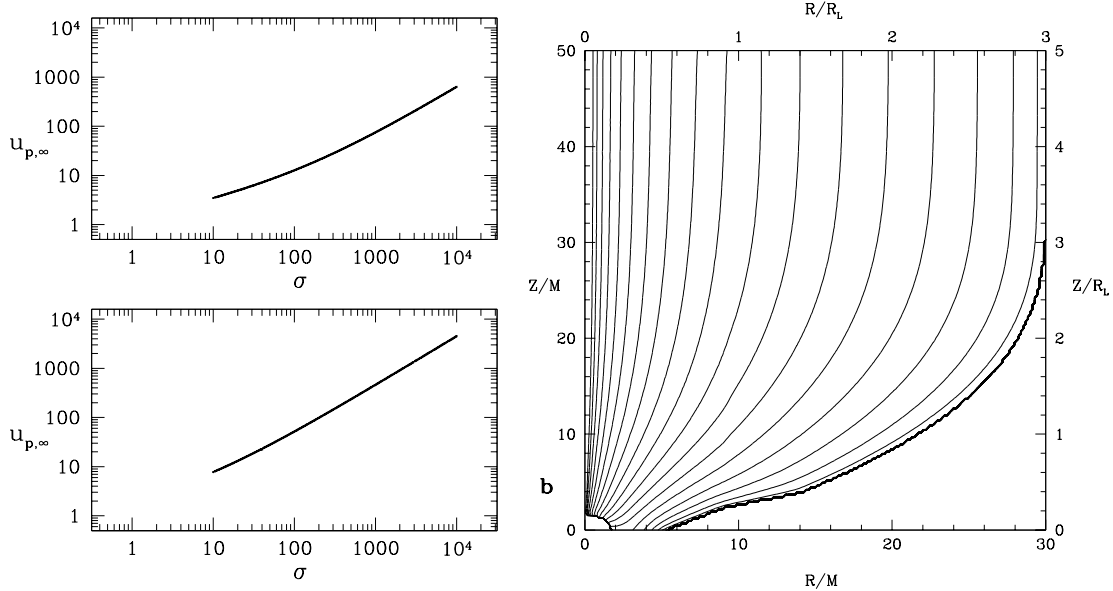


Figure 4: (Left) Modified Michel-scaling, $u_{p,\infty}(\sigma)$ for $B_p R^2 \sim R^{-0.01}$ (top) and $\sim R^{-0.1}$ (bottom). (Right) Global magnetic field structure of the collimation jet $\Psi(R, Z)$.

3.3 Collimation

Figure 3 shows a solution of the force-free GSE extending from the inner l.c. close to the hole, across the outer l.c. to the asymptotic, cylindrically collimated jet ($a = 0.8$, $\Psi_{\max} = 10^{21} \text{G cm}^2$, $I_{\max} = 10^{15} \text{A}$, $R_L = 10^7 \text{cm}$). The shape of the collimating jet is determined by the l.c. regularity condition. The field structure close to the hole and disk indicates a hollow jet with the bulk of the mass flow in the outer jet layers [16].

3.4 MHD jets in GRBs – open questions

The numerical solutions presented here show that the classical MHD jet formation scenario can indeed be extended to GRB parameter in order to achieve both ultra-relativistic velocities and strong collimation. However, serious questions remain unanswered, among them: (i) Due to the Michel-scaling, it is difficult to account for a wide range in Lorentz factors, $10^2 < \Gamma < 10^5$, which seems to be needed to generate the temporal variability of GRBs. (ii) Also, the bimodal distribution of GRB duration does not fit into the single MHD jet model. It is not clear, how such questions can be answered within a MHD jet model or whether pure electromagnetic or plasma processes are actually dominant.

Acknowledgments. I thank NORDITA for the financial support.

References

- [1] Mirabel, I.F., Rodriguez, L.F., 1994, Nature, 371, L46
- [2] Mundt, R., Ray, T.P., Bührke, T., Raga, A.C., Solf, J., 1990, A&A, 232, 37
- [3] Blandford, R.D., Payne, D.G., 1982, MNRAS, 199, 883
- [4] Camenzind, M., 1986, A&A, 162, 32
- [5] Fendt, C., Camenzind, M., 1996, A&A, 313, 591
- [6] Heyvaerts, J., Norman, C.A., 1989, ApJ, 347, 1055
- [7] Ouyed, R., Pudritz, R.E., 1997, ApJ, 482, 712
- [8] Uchida, Y., Shibata, K., 1985, PASJ, 37, 515
- [9] Koide, S., Shibata, K., Kudoh, T., 1998, ApJ, 495, L63
- [10] Okamoto, I., 1992, MNRAS 254, 192
- [11] Takahashi, M., Nitta, S., Tatematsu, Y., Tomimatsu, A., 1990, ApJ, 363, 206
- [12] Fendt, C., Greiner, J., 2001, A&A, 369, 308
- [13] Michel, F.C., 1969, ApJ, 158, 727
- [14] Begelman, M.C., Li, Z.-Y., 1994, ApJ 426, 269
- [15] Narayan, R., Yi, I., 1995, ApJ, 452, 710
- [16] Fendt, C., 1997, A&A, 319, 1025

Discussion

Blackman: Can you comment on the claims of Ustyugova et al. that the boundary shape strongly influences the presence or absence of collimation?

Fendt: We did not encounter this problem, maybe due to different boundary conditions in ZEUS code. Certainly, Ustyugova et al.'s point should be carefully considered.

Hujeirat: Do you predict the existence of a super-Keplerian layer above the disk, especially as you said you do agree with the Blandford & Payne 1982 scenario?

Fendt: The sub-Alfvénic disk wind co-rotates with the magnetic field. The toroidal velocity increases linearly $v_\phi \sim R$ along the flow. Beyond the Alfvén point, $v_\phi \sim R^{-1}$.